IRIS AperTO

UNIVERSITÀ DEGLI STUDI DI TORINO

AperTO - Archivio Istituzionale Open Access dell'Università di Torino

**Mapping Soil Water Capacity Through EMI Survey to Delineate Site-Specific Management Units Within an Irrigated Field**

**This is a pre print version of the following article:**

*Original Citation:*

*Availability:*

This version is available http://hdl.handle.net/2318/1619619 since 2016-12-01T14:00:08Z

*Published version:*

DOI:10.1097/SS.0000000000000159

*Terms of use:*

Open Access

Anyone can freely access the full text of works made available as "Open Access". Works made available under a Creative Commons license can be used according to the terms and conditions of said license. Use of all other works requires consent of the right holder (author or publisher) if not exempted from copyright protection by the applicable law.

(Article begins on next page)

17 September 2024

# Mapping soil water capacity through EMI survey to delineate site specific management units within an irrigated field

*Ortuani Bianca*

Researcher, Università degli Studi di Milano, Dipartimento di Scienze Agrarie ed Ambientali, via Celoria 2, 20133 Milano, Italy, fax +39 02 50316911, tel. +39 02 50316905, e-mail bianca.ortuani@unimi.it

*Chiaradia Enrico Antonio*

Researcher, Università degli Studi di Milano, Dipartimento di Scienze Agrarie ed Ambientali, via Celoria 2, 20133 Milano, Italy, fax +39 02 50316911, tel. +39 02 50316913, e-mail enrico.chiaradia@unimi.it

*Priori Simone*

Researcher, Consiglio per la Ricerca in Agricoltura e l'Analisi dell'Economia Agraria - Research Centre for Agrobiology and Pedology (CREA-ABP), piazza M. d'Azeglio 30, 50121 Firenze, Italy, fax +39 055 2480903, tel. +39 055 249127, e-mail simone.priori@crea.gov.it

*L'Abate Giovanni*

Technologist, Consiglio per la Ricerca in Agricoltura e l'Analisi dell'Economia Agraria - Research Centre for Agrobiology and Pedology (CREA-ABP), piazza M. d'Azeglio 30, 50121 Firenze, Italy, fax +39 055 2480903, tel. +39 055 2491221, e-mail giovanni.labate@crea.gov.it

*Canone Davide*

Researcher, Politecnico e Università di Torino, Dipartimento Interateneo di Scienze Progetto e Politiche del Territorio, viale Mattioli 39, 10125 Torino, Italy, fax +39 011 0907429, tel. +39 011 0907428, e-mail davide.canone@unito.it

*Comunian Alessandro*

Researcher, Università degli Studi di Milano, Dipartimento di Scienze della Terra "A.Desio", via Cicognara 7, 20129 Milano, Italy, fax +39 02 50318489, tel. +39 02 50318481, e-mail alessandro.comunian@unimi.it

*Giudici Mauro*

Full professor, Università degli Studi di Milano, Dipartimento di Scienze della Terra "A.Desio", via Cicognara 7, 20129 Milano, Italy, fax +39 02 50318489, tel. +39 02 50318478, e-mail mauro.giudici@unimi.it

CINFAI, piazza Niccolò Mauruzi 17, 62029 Tolentino (MC), Italy

CNR-IDPA, via Mario Bianco 9, 20131 Milano, Italy

*Mele Mauro*

Researcher, Università degli Studi di Milano, Dipartimento di Scienze della Terra "A.Desio", via Cicognara 7, 20129 Milano, Italy, e-mail mauro.mele@unimi.it

*Facchi Arianna*

Researcher, Università degli Studi di Milano, Dipartimento di Scienze Agrarie ed Ambientali, via Celoria 2, 20133 Milano, Italy, fax +39 02 50316911, tel. +39 02 50316909, e-mail arianna.facchi@unimi.it

**Running title:** Mapping soil water capacity through EMI survey

**Funding:** This research was funded by the Department of Agricultural and Environmental Sciences of the University of Milan (UNIMI) through the Development Plan UNIMI 2014 and, partially, by the Italian Ministry of Education, Universities and Research, through the Italian Research Project of Relevant Interest (PRIN) 2010-2011, prot. 20104ALME4: "National network for monitoring, modelling, and sustainable management of erosion processes in agricultural land and hilly-mountainous area" (PI Mario Aristide Lenzi).

**Abstract**

An accurate and high-resolution mapping of soil properties allows optimizing the management of irrigation and fertilization at field scale, by applying variable amounts of water and nutrients. The site-specific management is fundamental to improve crop yield and to use resources more efficiently, improving the environmental sustainability.

The adoption of site-specific management practices requires the delineation in the field of sub-regions with similar soil properties affecting yield (Site Specific Management Units, SSMU). It is common practice to characterize the spatial variability of soil properties through electromagnetic induction (EMI) surveys, to obtain soil electrical conductivity (EC) maps which can be used to delineate SSMUs.

The objectives of this work, carried out over an uniformly drip irrigated and fertilized maize, were: i) delineating SSMUs from EC maps; ii) comparing the SSMUs inferred from measurements with two different EMI sensors ; iii) mapping the soil available water-holding capacity (AWC) from EC maps through a regression model between EC and measured AWC; iv) evaluating the significant differences of crop yield among the SSMUs.

The EC maps at increasing depths were processed through principal component analysis and three SSMUs were delineated for both EMI sensors using MZA software. The significant difference in crop yield across the three SSMUs, tested through the analysis of variance, suggested that AWC was the main limiting factor in crop yield. This result highlights the importance of a variable rate irrigation based on SSMUs, which could be a solution to save water and increase crop yield.

**Keywords**

soil electrical resistivity, soil proximal EMI survey, soil available water-holding capacity, site specific management units, irrigation management

## Introduction

The improvement in crop yield, both in quantity and quality, depends on the adoption of appropriate management strategies. In precision agriculture (PA), an effective management should take into account the spatial variability of soil conditions, plant development and crop yield within agricultural fields through the adoption of site-specific (SS) agricultural practices, consisting in variable rate applications of the agricultural inputs (i.e. water and nutrients), as a function of the spatial variability of soil and plant conditions. Moreover, the adoption of SS management practices is fundamental, not only to improve crop yield, but also

for a more efficient use of nutrients and irrigation water, and thus to increase the environmental sustainability of agricultural production.

The SS management requires detailed information to characterize the within-field spatial variability of soil properties, plant and crop yield and to delineate homogeneous sub-regions with similar yield limiting factors or similar soil properties affecting yield (Site Specific Management Units, SSMU). The traditional method to acquire information on the within-field variability is based on soil sampling at spatially distributed points, measuring the soil properties affecting yields with analytic methods (e.g., texture, soil organic matter, pH, water retention), and finally interpolating the data with geostatistical tools to produce detailed maps of the soil properties. This approach is extremely time-consuming.

In PA, the intensive and relatively time-saving measurements of soil Electrical Conductivity (EC) acquired through non-invasive geophysical proximal soil sensors are commonly used to create quick and high resolution soil maps, useful to delineate SSMU (*Corwin et al*., 2003; *Morari et al*., 2009; *Moral et al*., 2010; *van Meirvenne*, 2013). The EM38mk2 (by Geonics Ltd, Mississauga, Ontario, Canada) and the Profiler-EMP400 (by Geophysical Survey Systems Inc., Nashua, New Hampshire, USA) are two Slingram ground-conductivity meters used in PA (*Doolittle and Brevik*, 2014) to measure EC with non-contact methods based on the principle of electromagnetic induction (EMI). The EM38mk2 is the most widely used EMI sensor in PA, while the Profiler-EMP400, a multi-frequency EMI sensor, is relatively new and still not largely applied. Because of the expanding use of the multi-frequency EMI sensors for a more effective assessment of the soil profile variability (*Triantafilis et al*., 2013), the comparison between the EC data collected with EM38mk2 and Profiler-EMP400 is an interesting issue to assess the reliability of the multi-frequency sensors to delineate SSMUs devoted to the optimization of agricultural practices. A comparison of the well-known EM38mk2 with multi-frequency EMI sensors as the Profiler-EMP400 (*Priori et al*., 2011) is still lacking in the PA literature, whereas some works compare EM38mk2 with other single frequency EMI sensors (*Gebbers et al*., 2009; *Saey et al*., 2009; *Saey et al*., 2011).

The cluster analysis of the data layers acquired through EMI sensors at increasing soil depths is one of the most common method to delineate SSMUs (*Ortega and Santibanez*, 2007; *Priori et al*., 2013). Particularly, a free software package implementing an unsupervised fuzzy classification method, the Management Zone Analyst (MZA, *Fridgen et al*., 2004), is commonly used in PA applications (*Moral et al*., 2010; *Scudiero et al*., 2013).

The recent literature highlights how the EC data are strongly correlated to soil physical parameters, such as soil texture (*Doolittle et al*., 2002; *Moral et al*, 2010), gravel content

(*Morari et al.* 2009), and bulk density (*Andrè et al*., 2012), as well as to soil hydrological parameters (*Godwin and Miller*, 2003; *Hedley and Yule*, 2009; *Hedley et al*., 2010; *Hedley et al*., 2013). Particularly, some studies (*Hedley and Yule*, 2009; *Hedley et al*., 2010; *Hedley et al*., 2013; *Priori et al*., 2013; *Fortes et al*, 2015) show the strong relation between the EC values and the total available water-holding capacity of the soil (AWC). The correlation between EC and AWC can be explained by the strong relationships of both the variables with soil physical features as texture, rock fragments, porosity, and bulk density (*Godwin and Miller*, 2003; *Priori et al*., 2013).

Some authors used this relation to predict AWC values from EC auxiliary data, thus obtaining high-resolution AWC maps from the EC maps derived through soil proximal monitoring with geophysical sensors (*Hedley et al*., 2010; *Fortes et al*, 2015). Since AWC is the available amount of water that can be stored in soil to be available for growing crops, a detailed knowledge of the within-field variability of AWC is extremely important to optimize irrigation by applying variable amounts of water according to the AWC spatial variability. When the soil water availability is the main limiting factor in crop yield, the variable-rate irrigation allows not only to save water but also to improve crop yield. This work was focusing on the issues concerning the delineation of SSMUs as proper tool to optimize the site-specific management of irrigation.

The main objectives of this study were: (i) to verify the effectiveness of obtaining an high-resolution AWC map from EC maps, by calibrating a linear regression model between EC values interpolated from data acquired with EMI sensors and AWC values obtained from laboratory measurements on collected soil samples in 15 points within the field (*Hedley et al*., 2009); (ii) to assess the correlation between AWC and EC to estimate the reliability of the delineation of SSMUs from EMI data as an effective tool to optimize the irrigation management practices and improve crop yield.

The specific objectives were: (i) to delineate the SSMUs from EC maps at increasing soil depths, by using MZA software; (ii) to compare the SSMUs delineated from EC maps produced with two different EMI sensors (EM38mk2 and Profiler-EMP400); (iii) to evaluate the significant differences of crop yield across the SSMUs; (iv) to predict high-resolution AWC map from EC map, to identify variables affecting crop yield.

## Materials and methods

### *The experimental site*

The experimental site is a 96 m × 192 m plot of sandy-loam soil located within an arable field in Northern Italy (Landriano – PV, 521109E 5018754N), 20 km south from Milan (Fig. 1a). It is situated in a flat area at about 90 m a.s.l., characterized by a semi-humid climate. The average values of the main climatic variables, calculated on the data recorded in the period 1997-2011 at an ARPA (Regional Environmental Protection Agency) agro-meteorological station installed less than 500 m from the experimental site, are reported in *Facchi et al.* (2013) and briefly summarized here: monthly total rain varies from approximately 40 mm in July to 100 mm in November, and monthly averages of the minimum and maximum air temperature vary respectively from approximately – 2 °C and 6 °C in January to 12 °C and 30 °C in July. Fig. 2 shows the behavior of daily mean temperature and rainfall registered during the monitoring period at the ARPA station.

According to the regional 1:250.000 soil map (http://www.geoportale.regione.lombardia.it), soils of the area are classified as "Aquultic Haplustalfs coarse loamy, mixed, mesic" (USDA, 1994) or "Stagnic Luvisol" (FAO, 1990), belonging to the land system of "fluvioglacial and fluvial main plain, filled during the last glacial period". The soils are usually coarse loamy in texture and characterized by a variable content of gravels, hydroximorphic features are frequent, and the drainage is moderate.

***EMI survey***

The monitoring activities were conducted from October 2014, after crop harvesting, to the end of the following cropping season in August 2015. The field was sowed with Zea-mays at the beginning of April 2015, and uniformly drip irrigated from July 2015 until the beginning of August 2015; the harvest was at the end of August 2015. .

EMI surveys were carried out at the end of October 2014, following a rainfall period of 15 days (with daily precipitation ranging from 0.5 mm to 32 mm), and 10 days after the last precipitation event (Fig. 2), when the bare soil water content may be supposed close to the field capacity. Two different EMI sensors were used and the dependence of their response with respect to the actual soil profile variability was assessed by comparing the EMI data with 2-D Electrical Resistivity Imaging (ERI) data. The ERI dataset was collected one day before the EMI survey date, along two perpendicular transects (Fig. 1a), following the main directions of soil variability.

Two easily-portable EMI proximal soil sensors, namely EM38mk2 (Fig. 1b) and Profiler-EMP400 (Fig. 1c) were used to map EC spatial variability within the experimental site. Hereinafter, these EMI sensors are denoted as EM38 and EMP400.

The EM38 is equipped with two receiving coils whose distances from the transmitting coil are equal to 0.5 m and 1 m, its operating frequency is 14.6 kHz and data are collected in vertical dipole orientation (VDO). Mc Neill (1990) demonstrated that the cumulative response of the measurement is a non-linear function, and the depth of investigation (DOI) of the instrument is about 0.75 m for the 0.5 m coil spacing, and 1.5 m for the 1 m coil spacing.

The EMP400 is a multi-frequency EMI sensor, which can collect data up to three frequencies from 1 kHz to 16 kHz, in horizontal and vertical dipole orientations (respectively HDO and VDO), with a coil spacing equal to 1.22 m. In this study, the EMP400 was used in VDO operating mode, with selected frequencies 5 kHz, 10 kHz and 15 kHz. The EMP400 is slightly more sensitive at larger depths than the EM38, because of the larger coils distance.

Site-specific calibration was carried out for both systems by keeping the systems in the air and on the ground according to the specifications made by the manufacturers.

For both EMI sensors, the EC measurements were acquired along 9 transects 12 m apart and parallel to the longer side of the plot; the survey data were acquired in continuous mode, approximately corresponding to a half-meter-long sampling spacing. The EM38 survey was performed with the instrument on a non-metallic cart pulled by an ATV quad (Fig. 1b); a GPS antenna with WAAS-EGNOS correction (accuracy approximately 3 m) was placed on the front of the cart. The EMP400, equipped with an integrated WAAS GPS, was carried by hand (Fig. 1c).

Since EC measurements depend on soil temperature (*Slavich and Petterson*, 1990), during the EMI and ERI surveys one soil temperature profile was continuously measured just outside the experimental plot by using four 107-L temperature sensors (Campbell Scientific, Inc., Logan, UT, USA) installed at the depths 10 cm, 20 cm, 50 cm and 70 cm.

The EC data collected with both EMI sensors were interpolated on a regular grid with 6 m spacing, by ordinary kriging (*Journel and Huijbregt*s, 1978). The parameters of the variogram models used to interpolate EC data were obtained through a fitting procedure based on the cross-validation performances provided in the R GSTAT package (*Pebesma*, 2004). The kriged values were smoothed by spline on a regular grid with 1 m spacing to filter out the effect of spike measurements.

Finally, the interpolated EC values were converted into electrical resistivity (ER) values, to compare EMI and ERI survey. Two ER maps were derived from the EM38 data, corresponding to the soil depths of about 0.75 m and 1.5 m, while three ER maps were derived from the EMP400 data, one for each selected frequency, corresponding to increasing soil depths with decreasing frequency.

***ERI survey***

ERI survey is a direct-current (DC) method that requires a computer-controlled multi-electrode system and metallic electrodes driven into the ground surface along a straight line at a constant electrode spacing (*Reynolds*, 2011; *Loke et al.*, 2013). The soil apparent electrical resistivity is obtained by measuring the voltage difference between a pair of receiving electrodes (potentiometric dipole) when an electrical field is applied by two source electrodes (current dipole) and by computing a geometrical factor dependent on the separation among the electrodes. The measurements are collected for a fixed quadripole (potentiometric dipole + current dipole) configuration by increasing the electrodes separation, thus producing apparent electrical resistivity values corresponding to increasing exploration depths.

The apparent resistivity measurements were acquired with a 48 channels 16SG24 georesistivity meter by PASI srl (Torino, Italy) along two perpendicular transects within the experimental plot (Fig. 1a), almost one-hundred-meters-long, with an average of 300 measurements quadripoles for each section. The measurements were acquired using a Wenner array with electrode spacing, $a$, equal to 2 m; the order of the array, i.e. the separation of a current electrode from the nearest potential electrode, was fixed at a maximum value equal to $5a$, so that the maximum exploration depth obtained was approximately 5 m below ground surface.

The apparent resistivity data were processed using the RES2DINV software (*Loke*, 1999; *Loke et al.*, 2003) to model the 2-D variability of the ER along the transects. A robust inversion routine (L1-NORM) using a least-square optimisation method (*Loke and Barker*, 1995) was adopted to highlight the subsurface regions separated by sharp boundaries and with approximately uniform electrical properties (*Loke et al.*, 2003).

***Local measurements***

Soil texture and water retention properties were measured in 15 points placed on a regular grid (Fig. 1a), while crop yields were monitored in 14 plots randomly distributed (Fig. 1a).

Soil samples were collected at two depths of 15 cm and 30 cm (two replicates, each) for a total amount of 60 samples both disturbed and undisturbed. Soil texture was measured on disturbed soil samples while undisturbed soil samples allowed measuring bulk density and soil water content at field capacity (FC) and wilting point (WP). FC and WP were measured by Richards apparatus, at 10 kPa and 1500 kPa, respectively. The volumetric soil moisture values FC and WP at depths of 15 cm and 30 cm were determined and averaged, finally

AWC was calculated by the difference of the two averaged values and considered as representative for the top 30 cm of soil.

Local EC values were measured in 7 points (Fig. 1a) by using the soil resistivity meter EC-probe (by Eijkelkamp, The Netherlands) at different depths down to 1 m. The EC-probe consists of a steel rod 110 cm long containig four ring-shaped electrodes separated by insulation rings. The outer electrodes are current electrodes, while the inner ones measure the voltage drop. The probe cone holds a temperature sensor for data correction.

***Crop yield measurements***

At the end of August 2015, the crop yield was measured in 14 plots randomly distributed (Fig. 1a). For each plot (2 m × 2 m), 21 plants were harvested and the maize cobs were separated and dried (for almost 30 hours in oven at 105 °C). The dry weight of maize grains was measured, and the mean value per plant was calculated. Finally, the dry weight per hectare was attained considering a planting density of 80000 plants/ha.

***Delineation of SSMUs***

The ER maps derived from EMI data corresponding to increasing DOIs are usually strongly correlated, since EMI measurements depend on the cumulative response of the whole investigated soil profile. On the other hand, all the ER maps related to the soil depths of agronomic interest include important information on the vertical variability of the soil, and then they should be considered to delineate the SSMUs. For these reasons, Principal Component Analysis (PCA) (*Jolliffe*, 2002) was carried out on the ER maps corresponding to soil depths up to almost 2 m below the ground surface, in order to produce new uncorrelated maps, which are the maps of the principal components (PC).

The maps of the selected PCs representing the greatest part of the total variability of the original correlated ER maps were considered to delineate the SSMUs by using MZA software.

The MZA software implements a fuzzy c-means unsupervised clustering method (*Odeh et al.*, 1992). This classification algorithm compares all the observations (an observation is the set of variables at a single sampling point) to each other and cluster the similar ones together, thus generating homogeneous zones. The zone delineation is based on a single variable or a combination of variables. The measure of similarity is the distance in the variable domain of all the observations from the cluster centroid. If the variables are uncorrelated (as in the case of PCs), the Euclidean distance can be used (*Moral et al.* 2010) and the similarity accounts

for the difference in the variable values; for correlated variables, the Mahalanobis distance (*Mahalanobis*, 1936) is used, accounting for differences in correlation behavior. According to the fuzzy method, the observations at the edges between zones can be members of more than one zone. This membership sharing is controlled by a fuzziness exponent greater than 1. The optimum number of zones depends on the fuzziness performance index (FPI) and the normalized classification entropy index (NCE). FPI measures the degree of separation between zones (the larger the FPI, the stronger is the membership sharing occurring among zones), and NCE measures the degree of disorganization created by identifying the zones (the larger the NCE, the higher is the amount of disorganization among zones). The optimum number of zones is reached when both indices are at the minimum values.

***Soil AWC mapping through auxiliary data***

The high-density ER data acquired with EMI surveys were used as auxiliary data to predict and map soil AWC considering a linear relationship between ER and AWC. In particular, since AWC values refer to the surface soil layer, 30 cm thick, the EM38 data corresponding to the soil depth of about 0.75 and the EMP400 data for 15 kHz frequency were considered. The existence of spatial autocorrelation among the regression residuals was tested to properly choose the methodology to map AWC, between regression kriging and regression modeling.

A linear regression model between AWC and ER values was tested and the accuracy of the regression was calculated by a leave-one-out cross validation. The coefficient of determination ($R^2$), the residuals and the root mean square error of prediction (RMSE) were calculated. The spatial autocorrelation among residuals was evaluated by Moran's I index, using ArcGis 9.1. This index measures the spatial autocorrelation of a datapoint set using Global Moran's I statistics (*Anselin and Rey, 1991*). This is a well-known statistics method to test the null hypothesis that the spatial autocorrelation of a variable is zero. If Moran's I is close to 0 and p-value is not statistically significant, the investigated variable is not spatial autocorrelated. On the contrary, Moran's I values close to 1 (or -1) and $p < 0.05$ demonstrate a high spatial autocorrelation of the variable.

## Results

***The ER maps***

The EC data collected with both EMI sensors were kriged (see Table 2 for the parameters of the variogram model) and finally converted into ER values (Fig. 3 and Fig. 4). In Tables 3

and 4 are reported the cross-validation results and the statistics of the kriging standard deviation maps. The variogram models are different for the two EMI sensors: the exponential model used for the EM38 maps describes a spatial variability with lower continuity with respect to the EMP400 maps whose variability is described with a spherical model. As a matter of fact, the ER maps show some differences in their spatial variability, due to the different DOI values characterizing the two EMI sensors. Moreover, the lower range values characterizing the EM38 variograms suggest that the EMI data acquired by EM38 are more sensitive to soil variability at local scale than those acquired by EMP400.

In order to properly interpret the ER maps derived from EMI data, the evaluation of the effective DOI of the EMI instruments is required. The ERI surveys, providing information on the soil vertical profile, allow to compare the response of the two different EMI instruments to the soil profile variability and to evaluate their effective DOI.

The modeled ERI sections (Fig. 5) were calculated by inversion of the two ERI pseudo-sections measured along the two transects showed in Fig. 1a. The inversion results were obtained with average relative errors between the experimental and the calculated apparent resistivities of 1.65% for the C3-C7 transect and 2.5% for the A5-E5 transect. The ERI sections are characterized by horizontal bodies with uniform electrical properties with a maximum thickness of 2 m, separated by lateral sharp boundaries. The surface layers appear to be more heterogeneous than the under-laying strata. The local water table is clearly depicted as a horizontal interface marked by a decrease of ER approximately at 3 m depth. Moreover, the low sensitivity of the ERI data with respect to the actual vertical heterogeneity of soils at depths below 1 m, due to the electrode spacing equal to 2 m, clearly appears by comparing the modeled ERI section in Fig. 5b with the ER values measured in points C4 and C7 (see Table 5), located 72 m apart from each other along one of the transect. Note that the ERI values have to be corrected for the soil temperature, with coefficient 0.76 for an average soil temperature equal to 13 °C during the monitoring time (*Keller and Frishcknecht*, 1966), to compare these values with the ER values locally measured with EC-probe.

The ER map derived from the EM38 measurements relative to the 0.5 m coil spacing (hereinafter the ‘shallow EM38-map’) has the highest values, even higher than those obtained from the EMP400 measurements at 15 kHz (hereinafter the ‘EMP400_15kHz-map’). The EMP400_15kHz-map (the EMP400-maps relative to 15 kHz and 10 kHz are quite similar) appears to be less sensitive than the shallow EM38-map to the soil heterogeneity characterising the surface layers of the stratigraphy depicted in the ERI profile (Fig. 5). Indeed the coil spacing of EM38 is shorter than that of EMP400, whereas the operating

frequencies are similar, so that the investigated soil depth for EMP400 is expected to be greater than that for EM38. Particularly, the comparison of the two maps with the electrostratigraphy inferred from the ERI sections, shows that the effective DOI value is about 1 m for the EM38 with coil spacing equal to 0.5 m and higher than 1.5 m for the EMP400 with frequency equal to 15 kHz.

The EMP400-map for the frequency 5 kHz (hereinafter the 'EMP400_5kHz-map') shows ER values higher than those in the EM38-map relative to the 1 m coil spacing (hereinafter the 'deep EM38-map'). This effect could be interpreted as a signature of the vertical variation of ER, because the coil spacing is similar for both sensors, but the investigated depth for the EMP400 is expected to be greater due to the lower operating frequency. The above remark is consistent with the ER values decreasing with depth in the ERI sections, if the DOI relative to the EMP400_5kHz-map is considered deeper than the bottom of the soil layer investigated with the ERI survey. Moreover, the comparison of the deep EM38-map with the electrostratigraphy desumed from the ERI sections shows that the effective value of DOI for the EM38 with coil spacing 1 m should be greater than 1.5 m.

Finally, the two EM38-maps and the EMP400-maps with frequencies 15 kHz and 10 kHz were related to soil depths of agronomical interest. On the other hand, the EMP400 map relative to 5 kHz seems to be referred to soil volumes too deep to be considered of agronomic interest.

***The SSMUs***

The ER maps related to soil depths of agronomical interest, i.e., with the exclusion of the EMP400_5kHz map, were considered for PCA. The results obtained for each EMI sensor are illustrated in Table 6 (EM-38) and Table 7 (EMP400). The correlation matrices show that $PC_1$ accounted for more than 80% of the total variances of the ER maps, precisely 83% and 97%, respectively for the EM38-maps and the EMP400-maps. These high percentages were due to the strong correlation between the ER maps, being the correlation coefficient equal to 0.66 and 0.94, respectively for the EM38-maps and the EMP400-maps. Only $PC_1$ was selected because the variance of $PC_2$ was less than 1 for both cases. Moreover, $PC_1$ was strongly correlated (correlation coefficients greater than 0.90 for EM38 and EMP400), with both ER maps at increasing depths.

The software package MZA was used to classify the $PC_1$ maps (both maps calculated from the ER data sets acquired respectively with EM38 and EMP400) into SSMUs. For this study case, the information given by FPI was considered more relevant than that given by NCE.

Thus the best number of SSMUs suggested by MZA was three for the case relative to the EM38 data, and two for the case relative to the EM38 data, as illustrated in Fig. 6c. As a matter of fact, the FPI value relative to the EM38 data set was the lowest for the number of zones equal to three while the NCE value was 0.0153 and 0.0174 (thus rather similar) for number of zones equal respectively to two and three. The FPI and NCE values relative to the EMP400 data set are the lowest when the number of zones was equal to two. Nevertheless, it was considered relevant that, for a number of zones equal to three the index values computed for the EMP400 and the EM38 data sets were very close. This behavior showed that a common optimal condition existed, therefore the optimal number of zones was considered equal to three also for the EMP400 data set. Overall, the SSMUs (delineated in Fig. 6a and Fig. 6b) were quite similar, except for the units C related to the highest ER values. This behavior was mainly due to the different ranges of the shallow ER values measured with the two sensors. The Kappa Index of Agreement (*Landis and Koch*, 1977) was evaluated to compare the classification maps in Fig. 6. The index value equal to 0.58 was significantly different from 0 (p-value almost 0), showing that the extent of agreement was not random and that a moderate agreement existed.

***The AWC maps***

The superficial AWC values measured at 15 sampling points within the field (Fig. 1a) are illustrated in Table 8. The data from all the sampling locations (i.e., 15 points) were considered to investigate the correlation between AWC and ER. The ER values were selected in the grid nodes closer to the sampling points.

Table 9 shows the results of the linear regression analysis carried out to model AWC from the interpolated ER values. The leave-one-out cross-validation was used to assess the model performance. The coefficient of determination $R^2$ was high (> 0.60) and the RMSE was much lower than the standard deviation of the AWC data (equal to 2.2, Table 8) for both cases, relative to the shallow EM38-map and the EMP400_15kHz-map. Moreover, Moran's Index was close to 0 and p-value was not statistically significant ($p > 0.40$), therefore the residual was not spatially autocorrelated and the linear regression modelling was a proper tool to predict AWC from the auxiliary ER data.

Finally, some outliers were rejected and the statistical significance of the regressive models calibrated with the available data (13 and 14 observations for the two cases, Fig. 7) was verified through the Fisher test ($p < 0.0002$). The $R^2$ value and the RMSE were respectively

0.74 and 1.1, for the case referring to the shallow EM38-map, and 0.84 and 0.9 for the case referring to the EMP400_15kHz-map.

The best regression model, that is the one showing the greatest $R^2$ value ($R^2$ = 0.84, in the specific case of the EMP400_15kHz-map), was selected to estimate the AWC values in the nodes of the 1 m grid, thus obtaining a high- resolution AWC map (Fig. 8a). Moreover, this regression model was selected because of the range of ER values used for the calibration, which included almost the whole range of the ER values in the EMP400_15kHz-map. Consequently, the prediction errors on AWC values, due to extrapolation (i.e. using a regression model to predict values outside the range of data considered for calibration), were limited.

Also the AWC map was classified into zones by using the MZA software (Fig. 8b). The best number of homogeneous zones suggested by MZA in this case was two (Fig. 8c), rather than the three obtained by classifying the $PC_1$ maps elaborated from EMI data (Fig. 6a,b).

***Crop yield differences across the SSMUs***

The optimal SSMU delineation was validated through ANOVA evaluating the significant differences of crop yield across the SSMUs. The mean crop yield for each zone was estimated considering at least four measurement plots located within the zone (Fig. 9). Following the splitting of the measurement plots among the zones, which is different for the SSMU delineated from EM38 and EMP400 data, two yield datasets were defined, each consisting of four observations within every zone. The results of ANOVA were reported in Table 10. The homogeneity of variances and the normality hypothesis for the two datasets were verified through the Bartlett test ($p > 0.46$) and the Shapiro-Wilk test ($p > 0.30$) respectively. The Fisher tests (Table 10) were significant (0.05 significance level) for both datasets. The multiple comparisons of means were carried out through the TuckeyHSD post-hoc test (Table 11). For both datasets, the mean crop yields were different, with significance level lower than 0.050 ($p < 0.043$) between zones “a” and “b”, and “a” and “c”, whereas they could not be considered different ($p > 0.580$) between zones “b” and “c”. This behavior suggests that the distinction between zones “b” and “c” had no significant effects on the crop yield. Differences in crop yield can be mainly attributed to the effects of soil water availability. As a matter of fact, the two homogeneous zones delineated from the AWC map (Fig. 8b) correspond to the SSMUs for which the mean crop yields were significantly different (Fig. 9a,b): approximately, zone 1 corresponds to zone “a”, while zone 2 corresponds to the merging of zones “b” and “c”.

## Discussion and conclusions

Two EMI sensors commonly used in PA, namely EM38 and EMP400, were used and compared to produce ER maps for SSMU delineation. The EM38 seemed to be more sensitive than the EMP400 to the local variability in the shallow soils. Nevertheless, the SSMUs delineated with MZA software by combining the data acquired with each EMI sensor were quite similar, with the exception of the units related to the highest values of ER at the surface. Although the differences were small, the results stressed that the knowledge about the response of EMI sensors with respect to the soil profile heterogeneity was crucial to properly delineate SSMUs. Specifically, a correct knowledge about the effective DOI of the EMI instruments is required, in particular for multi-frequency sensors whose operating frequencies (which influence DOI) can be selected by users. Since in the scientific literature on PA there is a lack of applications with Profiler-EMP400, further researches will be necessary to describe correctly the response of the instrument to the soil profile heterogeneity.

The MZA software was used to delineate the SSMUs from ER maps related to increasing soil depths. In this case, the results stressed that the pre-processing of data with PCA was required not only to summarize the information on total variability (*Moral et al.*, 2010; *Van Meirvenne et al.*, 2013), but also to properly measure the similarity among point locations, in order to classify the ER data and to delineate SSMUs. As a matter of fact, MZA classifies the ER data by considering both the correlation among ER maps corresponding to different soil depths and the spatial variability of each ER map. Consequently, when the measure of similarity is the correlation among ER maps (i.e. Mahalanobis distance) the classification results could be misleading if the different behaviour in correlation among ER maps is related to a component with a negligible variability in each ER maps. The analysis dealing with components representing correlation among ER maps can be carried out through PCA. The PCA results showed that $PC_2$ accounted for the opposite behaviour in correlation among ER maps and represented a negligible percentage of the total ER variability. In this case the Mahalanobis distance was not considered for the classification by MZA. Finally, a pre-processing of ER maps at increasing depths through PCA is required to properly delineate SSMUs by MZA.

The SSMUs delineated through classification algorithms based on ER data only should be tested as proper tools to improve the crop yield. Particularly, this analysis is useful when yield maps are not available to define SSMUs (*Van Meirvenne et al.*, 2013). In our work, crop yield was measured locally in some plots and significant differences in crop yield across

the three SSMUs delineated by MZA was tested with ANOVA. The tests suggested that the classification in two SSMUs corresponds to significant differences in crop yield.

A high-resolution AWC map was produced by predicting the AWC values from the auxiliary data of an ER map, through a linear regression model calibrated with the observations in just 14 points. Particularly, the results concerning the strong correlation between AWC and ER values are really encouraging. The high values of the correlation coefficient (absolute values greater than 0.85) agree with the research studies shown in some recent papers (*Hedley and Yule*, 2009; *Fortes et al.*, 2015). The strong correlation between AWC and ER values stressed how the EMI surveys on bare soils are proper and reliable tools to classify the within-field variability of soil in different homogeneous zones for the site specific management of irrigation. Furthermore, the high-resolution AWC map were used to assess the SSMUs as tools to identify factors limiting crop yield in some zones and to improve the crop yield through variable rate irrigation. Indeed the AWC map was classified into two zones by using MZA, corresponding to the SSMUs with significant differences in crop yield. These results suggested that AWC was the main limiting factor in crop yield, thus stressing how variable rate irrigation could be a solution to save water and increase crop yield.

Since the regression model to produce the AWC map is valid in the range of the EC values used to calibrate the model, we think that our results could have been more meaningful if the soil sampling positions had been selected to investigate the full range of the ER values in the maps produced with both EMI sensors. Indeed the distinction on three SSMUs was more evident considering the ER maps elaborated from the EM38 data, but the regression model to produce AWC from the shallow EM38 map was not valid.

REFERENCES

André F., van Leeuwen C., Saussez S., Van Durmen R., Bogaert P., Moghadas D., de Rességuier L., Delvaux B., Vereecken H., Lambot S. 2012. High-resolution imaging of a vineyard in south of France using ground penetrating radar, electromagnetic induction and electrical resistivity tomography. J. Appl. Geophys. 78: 113-122.

Anselin, L. and Rey S. 1991. Properties of tests for spatial dependence in linear regression models. Geographical Analysis. 23**:** 112–131

Corwin D.L., Lesch S.M., Shouse P.J., Soppe R., Ayars J.E. 2003. Identifying Soil Properties that Influence Cotton Yield Using Soil Sampling Directed by Apparent Soil Electrical Conductivity. Agron. J. 95: 352-364.

Doolittle J.A., Indorante S.J., Potter D.K., Hefner S.G., McCauley W.M. 2002. Comparing three geophysical tools for locating sand blows in alluvial soils of Southeast Missouri. J. Soil Water Conserv. 57: 175-182.

Doolittle J.A. and Brevik E.C. 2014. The use of electromagnetic induction techniques in soil studies. Publications from USDA-ARS/UNL Faculty. Paper 1462.

Facchi A., Gharsallah O., Corbari C., Masseroni D., Mancini M., Gandolfi C. 2013. Determination of maize crop coefficients in humid climate regime using the eddy covariance technique. Agr. Water Manage. 130: 131-141

Fortes R., Millán S., Prieto M. H., Campillo C. 2015. A methodology based on apparent electrical conductivity and guided soil samples to improve irrigation zoning. Precis. Agric. DOI 10.1007/s11119-015-9388-7.

Fridgen J.L., Kitchen N.R., Sudduth K.A., Drummond S.T., Wiebold W.J., Fraisse C.W. 2004. Management zone analyst (MZA): Software for sub-field management zone delineation. Agron. J. 96:100-108.

Gebbers R., Lück E., Dabas M. 2009. Comparing of instruments for geoelectrical soil mapping at the field scale. Near Surface Geophysics 7(3):179-190

Godwin R.J., Miller P.C.H. 2003. A review of the technologies for mapping within-field variability. Biosyst. Eng. 84(4): 393-407.

Hedley C.B. and Yule I.J. 2009. A method for spatial prediction of daily soil water status for precise irrigation scheduling. Agr. Water Manage. 96(12): 1737-1745.

Hedley C.B., Bradbury S., Ekanayake J., Yule I.J. and Carrick S. 2010. Spatial irrigation scheduling for variable rate irrigation. Proceedings of the New Zealand Grassland Association 72: 97-102

1 Hedley C. B., Roudier P., Yule I. J., Ekanayake J., Bradbury S. 2013. Soil water status and
2 water table depth modelling using electromagnetic surveys for precision irrigation
3 scheduling. Geoderma. 199: 22-29.

4 Journel A.G.and Huijbregts C.J. 1978. Mining Geostatistics. Academic Press Inc.,London

5 Keller G.V., Frischknecht F.C. 1966. Electrical methods in geophysical prospecting.
6 Pergamon Press, Oxford

7 Landis JR, Koch GG. 1977. The measurement of observer agreement for categorical data.
8 Biometrics. 33: 159-174.

9 Loke M.H.. 1999. RES2DINV Rapid 2-D Resistivity and IP inversion using the least squares
10 method. Manual, Geotomo Software, Penang, Malaysia.

11 Loke M.H. and Barker R.D. 1995. Least-squares deconvolution of apparent resistivity
12 pseudosections. Geophysics. 60: 1682–1690.

13 Loke M.H., Acworth I., Dahlin T. 2003. A comparison of smooth and blocky inversion
14 methods in 2D electrical imaging surveys. Explor Geophys. 34: 182-187.

15 Loke M.H., Chambers J.E., Rucker D.F., Kuras O., Wilkinson P.B. 2013. Recent
16 developments in the direct-current geoelectrical imaging method. J. Appl. Geophys. 95: 135-
17 156.

18 Mahalanobis P.C. 1936. On the generalised distance in statistics. In Proceedings by National
19 Institute of Science of India. 2: 49-55.

20 McNeil, J.D., 1990. Geonics EM38 Ground Conductivity Meter: EM38 Operating Manual.
21 Geonics Limited, Ontario, Canada.

22 Moral F.J., Terron J.M., Marques da Silva J.R. 2010. Delineation of management zones using
23 mobile measurements of soil apparent electrical conductivity and multivariate geostatistical
24 techniques. Soil Till. Res. 106: 335–343.

25 Morari F., Castrignanò A., Pagliarin C. 2009. Application of multivariate geostatistics in
26 delineating management zones within a gravelly vineyard using geo-electrical sensors.
27 Comput. Electron. Agr. 68: 97-107.

1 Ortega R.A. and Santibanez O.A. 2007. Determination of management zones in corn (Zea
2 mays L.) based on soil fertility. Comput. Electron. Agr. 58: 49-59.

3 Pebesma E.J. 2004. Multivariable geostatistics in S: the gstat package. Computers &
4 Geosciences. 30(7): 683-691

5 Priori S., Martini E., Costantini E.A.C. 2011. Three proximal sensors for mapping skeletal
6 soils in vineyards. 19th World Congress of Soil Science, Soil solutions for a Changing World,
7 Brisbane, Australia. 121-124.

8 Priori S., Martini E., Andrenelli M.C., Magini S., Agnelli A.E., Bucelli P., Biagi M.,
9 Pellegrini S., Costantini E.A.C. 2013. Improving wine quality through harvest zoning and
10 combined use of remote and soil proximal sensing. Soil Sci. Soc. Am. J. 77(4): 1338-1348.

11 Reynolds J.M. 2011. An Introduction to Applied and Environmental Geophysics, 2nd
12 Edition. John Wiley & Sons, Inc., ISBN: 978-0-471-48535-3, pp 710.

13 Saey T., Simpson D., Vermeersch H., Cockx L., Van Meirvenne M. 2009. Comparing the
14 EM38DD and DUALEM-21S sensors for depth-to-clay mapping. Soil Sci. Soc. Am. J..
15 73(1): 7-12.

16 Saey T., Van Meirvenne M., De Smedt P., Cockx L., Meerschman E., Islam M.M., Meeuws
17 F. 2011. Mapping depth-to-clay using fitted multiple depth response curves of a proximal
18 EMI sensor. Geoderma. 162: 151-158.

19 Scudiero E., Teatini P., Corwin D.L., Deiana R., Berti A., Morari F. 2013. Delineation of
20 site-specific management units in a saline region at the Venice Lagoon margin, Italy, using
21 soil reflectance and apparent electrical conductivity. Comput. Electron. Agr. 99: 54-64.

22 Slavich P.G., Petterson G.H. 1990. Estimating average rootzone salinity from
23 electromagnetic induction (EM-38) measurements. Soil Research. 28(3): 453-463.

24 Triantafilis J., Terhune C.H., Monteiro Santos F.A. 2013. An inversion approach to generate
25 electromagnetic conductivity images from signal data. Environ. Model. Softw. 43: 88-95.

26 Van Meirvenne M., Islam M.M., De Smedt P., Meerschman E., Van De Vijver E., Saey T.
27 2013. Key variables for the identification of soil management classes in the aeolian
28 landscapes of north–west Europe. Geoderma. 199: 99–105.

***Figure 1*** *(a) The experimental plot, located in Northern Italy south of Milan and the experimental design; (b) the EMI sensor EM38mk2; (c) the EMI sensor Profiler-EMP400*

***Figure 2*** *Daily mean air temperature, T [°C], and precipitation, P [mm] at the experimental site during the monitoring period*

***Figure 3*** *Spatial distributions of the electrical resistivity (Ω m) measured with EM38 (VDO mode): (a) map relative to coil spacing 0.5 m; (b) map relative to coil spacing 1 m*

***Figure 4*** *Spatial distributions of the electrical resistivity (Ω m) measured with EMP400 (VDO mode), maps relative to frequencies: (a) 15 kHz; (b) 10 kHz ; (c) 5 kHz*

***Figure 5*** *Results of the ERI surveys: 2-D resistivity sections of electrical resistivity (Ω m) obtained along two perpendicular transects: (a) transect from approximately point A5 (at 0 m distance along the transect) to point E5 (at 94 m distance along the transect); (b) transect from point C3 (at 0 m distance along the transect) to point C7 (at 94 m distance along the transect)*

***Figure 6*** *Delineation of the SSMUs with MZA software, based on the map of the first principal component $PC_1$ elaborated from the data set collected through: (a) EM38; (b) EMP400; (c) fuzziness performance index (FPI) and normalized classification entropy index (NCE) as function of the number of zones*

***Figure 7*** *Linear regression of the total available water-holding capacity AWC values (%), estimated as the difference between volumetric soil moisture values at field capacity and wilting point, on the soil electrical resistivity ER values (Ωm) calculated from the EMI data, referring to: (a) the shallow EM38-map; (b) the EMP400-map (frequency 15kHz)*

***Figure 8*** *(a) Spatial distribution of the total available water-holding capacity AWC values (%), evaluated from the ER map referring to the EMP400 measurements with frequency 15kHz, through the calibrated regressive model defined in Fig.7b. (b) Delineation of homogeneous zones with MZA software, based on the AWC map. (c) Fuzziness performance*

*index (FPI) and normalized classification entropy index (NCE) as function of the number of zones*

***Figure 9*** *Localization within the SSMUs of plots for the crop yield measurements. SSMUs are respectively delineated from data sets collected by: (a) EM38; (b) EMP400*

***Table 1***. *Textural properties of the soil within the experimental plot (statistics over 15 sampling points): percentage [%] of sand, silt and clay*

***Table 2***. *Parameters of the variogram models used to interpolate the EC data through ordinary kriging. The data collected with EM38 are relative to the coil spacing equal to 0.5 m (shallow data) and 1 m (deep data), The EMI data collected with EMP400 are relative to the frequencies 15 kHz, 10 kHz and 5 kHz. Ranges for exponential models are to be considered as practical ranges*

***Table 3.*** *Results of the cross-validation procedure to fit the variogram models used to interpolate the EC data through ordinary kriging. The statistics of the standardized errors (i.e. the error divided by the kriging standard deviation) are reported. The data collected with EM38 are relative to the coil spacing equal to 0.5 m (shallow data) and 1 m (deep data), The EMI data collected with EMP400 are relative to the frequencies 15 kHz, 10 kHz and 5 kHz.*

***Table 4***. *Statistics of the kriging standard deviation maps obtained through the interpolation of the EC data. The data collected with EM38 are relative to the coil spacing equal to 0.5 m (shallow data) and 1 m (deep data), The EMI data collected with EMP400 are relative to the frequencies 15 kHz, 10 kHz and 5 kHz.*

***Table 5***. *Standard ER values (Ω m), referring to the temperature 25°C, locally measured with EC-probe*

***Table 6***. *PCA of the EM38-maps related to the soil depths of agronomical interest (both the ER maps):correlation matrix and variances of the standardised ER and the PCs. The shallow and deep ER maps refer to a coil spacing equal to 0.5 m and 1 m, respectively*

***Table 7***. *PCA of the EMP400-maps related to the soil depths of agronomical interest (only the ER maps with frequencies 15 kHz and 10 kHz). Correlation matrix and variances of the standardised ER and the PCs.*

***Table 8***. *Hydrological properties of the soil within the experimental plot (statistics over 15 sampling points): volumetric soil moisture values [-] at the field capacity (FC) and at the wilting point (WP); total available water-holding capacity (AWC), AWC = FC - WP*

***Table 9***. *Results of the linear regression analysis to predict AWC from ER values (data referring to all the 15 sampling locations). Leave-one-out cross-validation was carried out*

***Table 10***. *ANOVA results (through the Fisher test) to evaluate the significant differences of mean crop yields (t ha$^{-1}$) across the SSMUs*

***Table 11***. *Comparisons of mean crop yields across the SSMUs. TuckeyHSD p-values are reported*

***Table 1***. *Textural properties of the soil within the experimental plot (statistics over 15 sampling points): percentage [%] of sand, silt and clay*

| | **Sand** | | | **Silt** | | | **Clay** | | |
|---|---|---|---|---|---|---|---|---|---|
| Depth | Mean (%) | St.dev. (%) | CV (%) | Mean (%) | St.dev. (%) | CV (%) | Mean (%) | St.dev. (%) | CV (%) |
| 15 cm | 59.9 | 1.6 | 2.6 | 31.7 | 1.4 | 4.3 | 8.4 | 0.8 | 10.1 |
| 30 cm | 60.1 | 1.8 | 3.0 | 30.2 | 1.6 | 5.2 | 9.7 | 1.6 | 16.0 |
| Mean | 60.0 | 1.7 | 2.8 | 30.9 | 1.6 | 5.3 | 9.1 | 1.4 | 15.4 |

***Table 2***. *Parameters of variogram models used to interpolate the EC data with the ordinary kriging. The data collected with EM38 are relative to the coil spacing equal to 0.5 m (shallow data) and 1 m (deep data), The EMI data collected with EMP400 are relative to the frequencies 15 kHz, 10 kHz and 5 kHz. Ranges for exponential models are to be considered as practical ranges*

| | **EM38** | | **EMP400** | | |
|---|---|---|---|---|---|
| | **Shallow** | **Deep** | **15 kHz** | **10 kHz** | **5 kHz** |
| Model | exponential | exponential | spherical | spherical | spherical |
| Nugget [(mS $m^{-1}$)$^2$] | 0.16 | 1.80 | 0.80 | 0.10 | 0.20 |
| Sill [(mS $m^{-1}$)$^2$] | 1.20 | 4.30 | 3.40 | 3.00 | 2.70 |
| Range (m) | 57 | 66 | 82 | 85 | 79 |

***Table 3.*** *Results of the cross-validation procedure to fit the variogram models used to interpolate the EC data through ordinary kriging. The statistics of the standardized errors (i.e. the error divided by the kriging standard deviation) are reported. The data collected with EM38 are relative to the coil spacing equal to 0.5 m (shallow data) and 1 m (deep data), The EMI data collected with EMP400 are relative to the frequencies 15 kHz, 10 kHz and 5 kHz.*

| | **EM38** | | **EMP400** | | |
|---|---|---|---|---|---|
| | **Shallow** | **Deep** | **15 kHz** | **10 kHz** | **5 kHz** |
| Min [-] | -5.308 | -6.613 | -3.232 | -6.486 | -6.999 |
| Max [-] | 7.855 | 5.689 | 3.342 | 3.701 | 6.156 |
| Mean [-] | 0.001 | -0.000 | -0.001 | -0.001 | -0.001 |
| Var [-] | 0.999 | 1.110 | 0.987 | 0.979 | 0.945 |

***Table 4***. *Statistics of the kriging standard deviation maps obtained through the interpolation of the EC data. The data collected with EM38 are relative to the coil spacing equal to 0.5 m (shallow data) and 1 m (deep data), The EMI data collected with EMP400 are relative to the frequencies 15 kHz, 10 kHz and 5 kHz.*

| | **EM38** | | **EMP400** | | |
|---|---|---|---|---|---|
| | **Shallow** | **Deep** | **15 kHz** | **10 kHz** | **5 kHz** |
| Min [mS $m^{-1}$] | 0.485 | 1.451 | 0.964 | 0.392 | 0.520 |
| Max [mS $m^{-1}$] | 0.772 | 1.690 | 1.088 | 0.706 | 0.756 |
| Mean [mS $m^{-1}$] | 0.606 | 1.554 | 1.028 | 0.562 | 0.643 |
| St.Dev. [mS $m^{-1}$] | 0.062 | 0.047 | 0.031 | 0.084 | 0.063 |

***Table 5**. Standard ER values (Ω m), referring to the temperature 25°C, locally measured with EC-probe*

| Depth | A1 | A4 | A7 | B3 | C1 | C4 | C7 |
|---|---|---|---|---|---|---|---|
| 15 cm | 517 | 296 | 586 | 246 | 394 | 266 | 196 |
| 35 cm | 235 | 198 | 228 | 358 | 253 | 285 | 261 |
| 50 cm | 486 | 193 | 217 | - | 239 | 378 | 318 |
| 75 cm | 365 | 103 | 198 | - | 255 | 536 | - |
| 100 cm | 300 | 100 | 161 | - | 446 | 593 | - |

***Table 6****. PCA of the EM38-maps related to the soil depths of agronomical interest (both the ER maps):correlation matrix and variances of standardised ER and PCs. The shallow and deep ER maps refer to a coil spacing equal to 0.5 m and 1 m, respectively*

| | **Shallow ER** | **Deep ER** | **$PC_1$** | **$PC_2$** |
|---|---|---|---|---|
| **Shallow ER** | 1 | 0.66 | 0.91 | -0.41 |
| **Deep ER** | | 1 | 0.91 | 0.41 |
| **$PC_1$** | | | 1 | 0 |
| **$PC_2$** | | | | 1 |
| **variance** | 1 | 1 | 1.66 | 0.34 |

***Table 7****. PCA of the EMP400-maps related to the soil depths of agronomical interest (only the ER maps with frequencies 15 kHz and 10 kHz). Correlation matrix and variances of standardised ER and PCs.*

| | **15 kHz-ER** | **10 kHz-ER** | **$PC_1$** | **$PC_2$** |
|---|---|---|---|---|
| **15 kHz-ER** | 1 | 0.94 | 0.99 | 0.17 |
| **10 kHz-ER** | | 1 | 0.99 | -0.17 |
| **$PC_1$** | | | 1 | 0 |
| **$PC_2$** | | | | 1 |
| **variance** | 1 | 1 | 1.94 | 0.06 |

***Table 8****. Hydrological properties of the soil within the experimental plot (statistics over 15 sampling points): volumetric soil moisture values [-] at the field capacity (FC) and at the wilting point (WP); total available water-holding capacity (AWC), AWC = FC - WP*

| | **FC** | | | **WP** | | | **AWC** | | |
|---|---|---|---|---|---|---|---|---|---|
| Depth | Mean (-) | St.dev. (-) | CV (%) | Mean (-) | St.dev. (-) | CV (%) | Mean (-) | St.dev. (-) | CV (%) |
| 15 cm | 29.6 | 2.3 | 7.6 | 10.0 | 0.9 | 8.7 | | | |
| 30 cm | 28.0 | 3.2 | 11.5 | 9.9 | 1.1 | 10.7 | | | |
| **Mean** | **29.0** | **2.4** | **8.3** | **10.0** | **0.8** | **8.1** | **18.9** | **2.2** | **11.6** |

***Table 9***. *Results of the linear regression analysis to predict AWC from ER values (data at all the sampling locations - 15 points - were considered). Leave-one-out cross-validation was carried out*

| | Regression model | $R^2$ | RMSE | Global Moran's I | p-value | Spatial correlation |
|---|---|---|---|---|---|---|
| **EM38** | -0.030 *x* + 27.98 | 0.61 | 1.6 | -0.18 | 0.49 | NO |
| **EMP400** | -0.047 *x* + 26.91 | 0.72 | 1.2 | 0.09 | 0.64 | NO |

***Table 10***. *ANOVA results (through the Fisher test) to evaluate the significant differences of mean crop yields (t ha$^{-1}$) across the SSMUs*

| | Mean yield zone a | Mean yield zone b | Mean yield zone c | F value | p-value |
|---|---|---|---|---|---|
| **EM38** | 12.5 | 10.3 | 9.5 | 8.28 | 0.009 |
| **EMP400** | 12.5 | 9.6 | 9.3 | 13.41 | 0.002 |

***Table 11****. Comparisons of mean crop yields across the SSMUs. TucheyHSD p-values are reported*

| | **Zones a-b** | **Zones c-a** | **Zones c-b** |
|---|---|---|---|
| **EM38** | 0.042 | 0.009 | 0.583 |
| **EMP400** | 0.005 | 0.003 | 0.921 |

*Dear **Referee 1** we would thank you for your reviews and also for your positive opinion on the paper. We have done our best to answer to your proper remarks concerning the improving of Methods section and the description of kriging results. We have shortened and simplified the Methods section, according to your comments.*
*Please find below the answers to your reviews.*

1. The authors in the abstract stated that "An accurate and high-resolution mapping of soil properties allows to optimize the management of irrigation and fertilization at field scale", but there is no mention about fertilization in the rest of the manuscript. This term should be omitted

*Actually in precision agriculture the high-resolution soil mapping and the subsequent zoning in homogeneous areas are tools to be used to optimize not only the irrigation management but also the nutrient management. In Introduction section we presented the issues related to both the management of irrigation and nutrients, moreover we highlighted that the paper is focusing on the issues concerning the delineation of homogeneous zones as proper tool to optimize the site-specific management of irrigation.*

2. The number and the measurements frequency of the monitoring parameters are confusing in many parts and should be clarified in methodology section.

*We have improved the organization of the Methods section, making it shorter and clearer. Therefore we think that the monitoring activities and measuremets have been more clearly presented*

3. Authors should clarify why they use the ordinary Kriging interpolation method to obtain raster maps for the study area. Also, they should give some statistical metrics of the resulting map. In 2d representation of the final kriging results the corresponding uncertainty should be also included.

*The use of geostatistical methods to interpolate the EC data has allowed not only to obtain the high-resolution soil maps, but also describe the spatial variability models (by the definition of the variogram) from which it was found that - as commented in the results - the measurements acquired with different EMI sensors have different spatial variability properties. Moreover Tables 3 and 4 have been added to describe the uncertainty of the kriging results.*

4. Moreover, authors should clarify why they did not use the drip irrigation network as secondary information for cokriging

*The drip irrigation was uniformly applied therefore the information about the irrigation network could not improve the interpolation results*

5. The authors mention many unnecessary information that lead to an extended manuscript, for instance (see page 10, lines 11-14). The manuscript should become shorten by half and this can be achieved organizing the methodology section. In addition, it is necessary to describe clearly the inputs that where used in the proposed methodology.

*We think the better organization of the Methods section made clearer the description of the inputs used in the proposed methodology.*

---

*Dear **Referee 2**, thank you for your positive evaluation of the paper. The English language has been further refined and the grammer has been improved, according to your comments.*

Figure

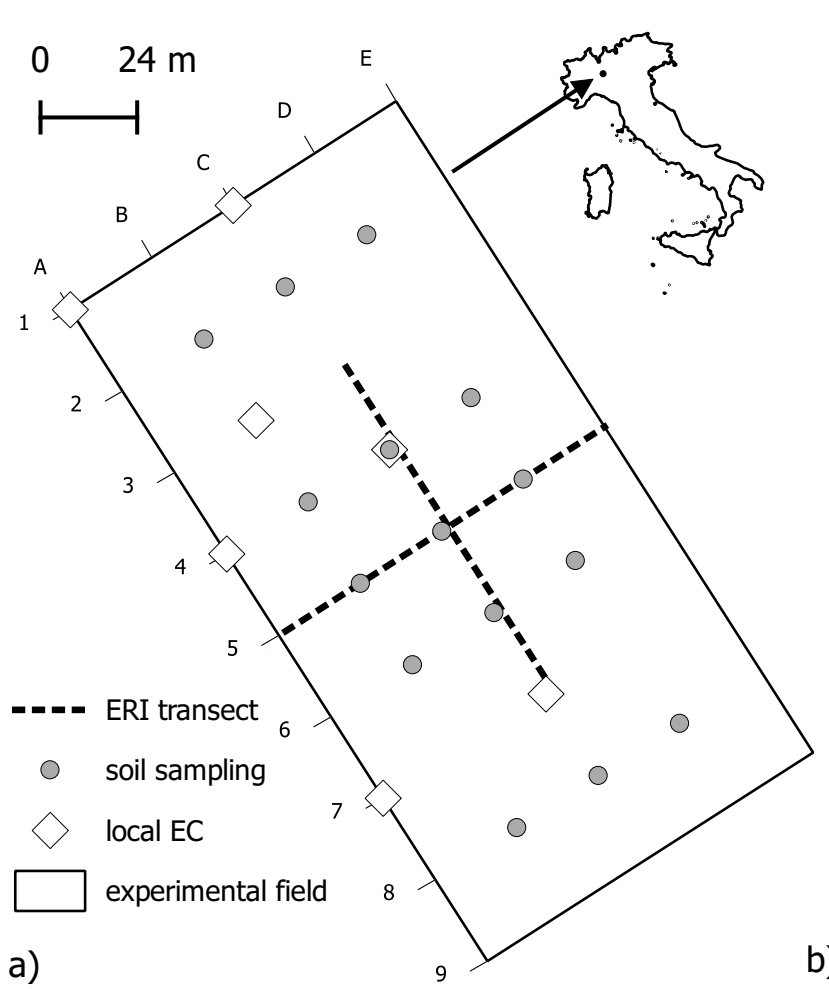
0
24 m
A
B
C
D
E
1
2
3
4
5
6
7
8
9
ERI transect
soil sampling
local EC
experimental field

a)

b)

c)

Figure

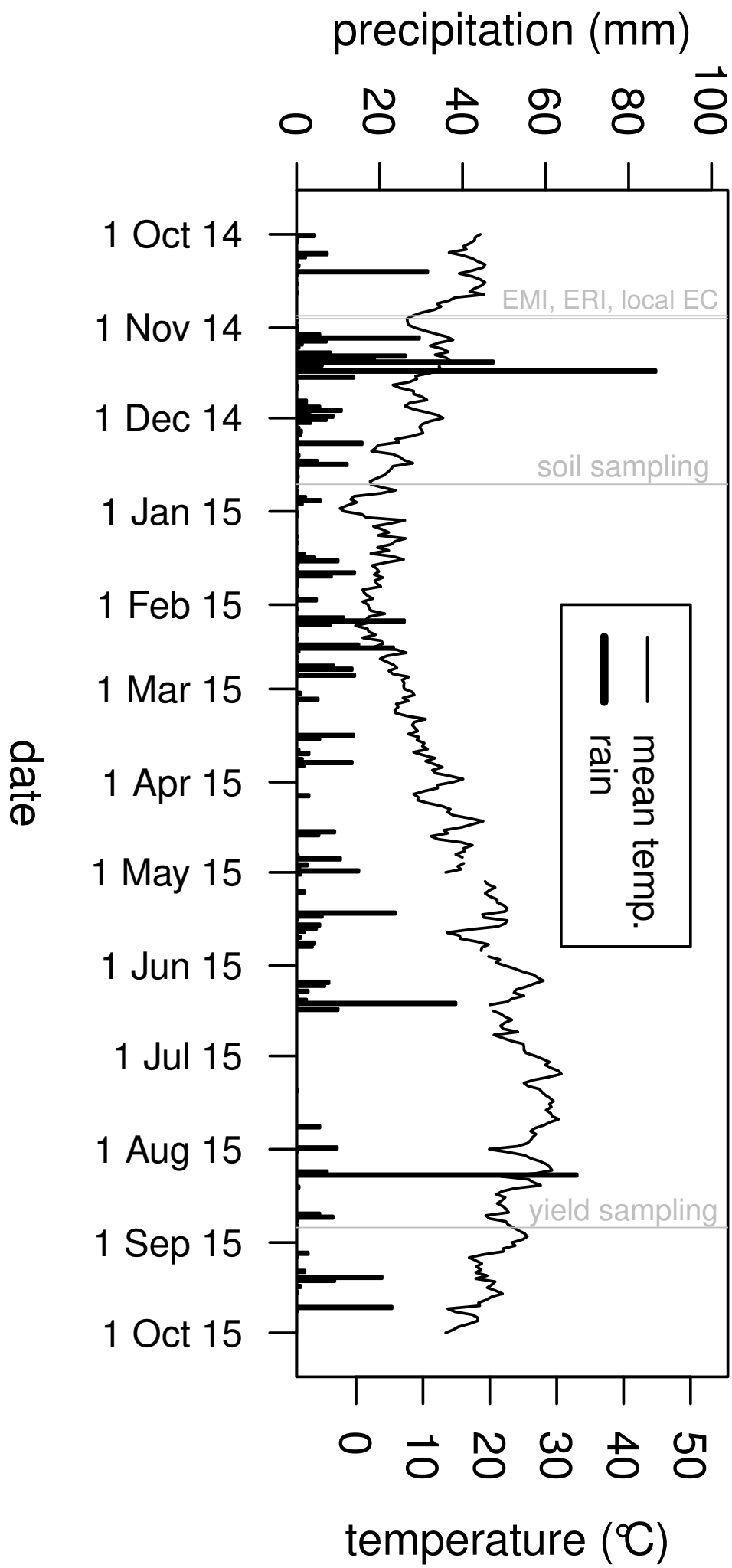
precipitation (mm)
0
20
40
60
80
100
1 Oct 14
1 Nov 14
1 Dec 14
1 Jan 15
1 Feb 15
1 Mar 15
1 Apr 15
1 May 15
1 Jun 15
1 Jul 15
1 Aug 15
1 Sep 15
1 Oct 15
date
EMI, ERI, local EC
soil sampling
yield sampling
mean temp.
rain
0
10
20
30
40
50
temperature (℃)

Figure

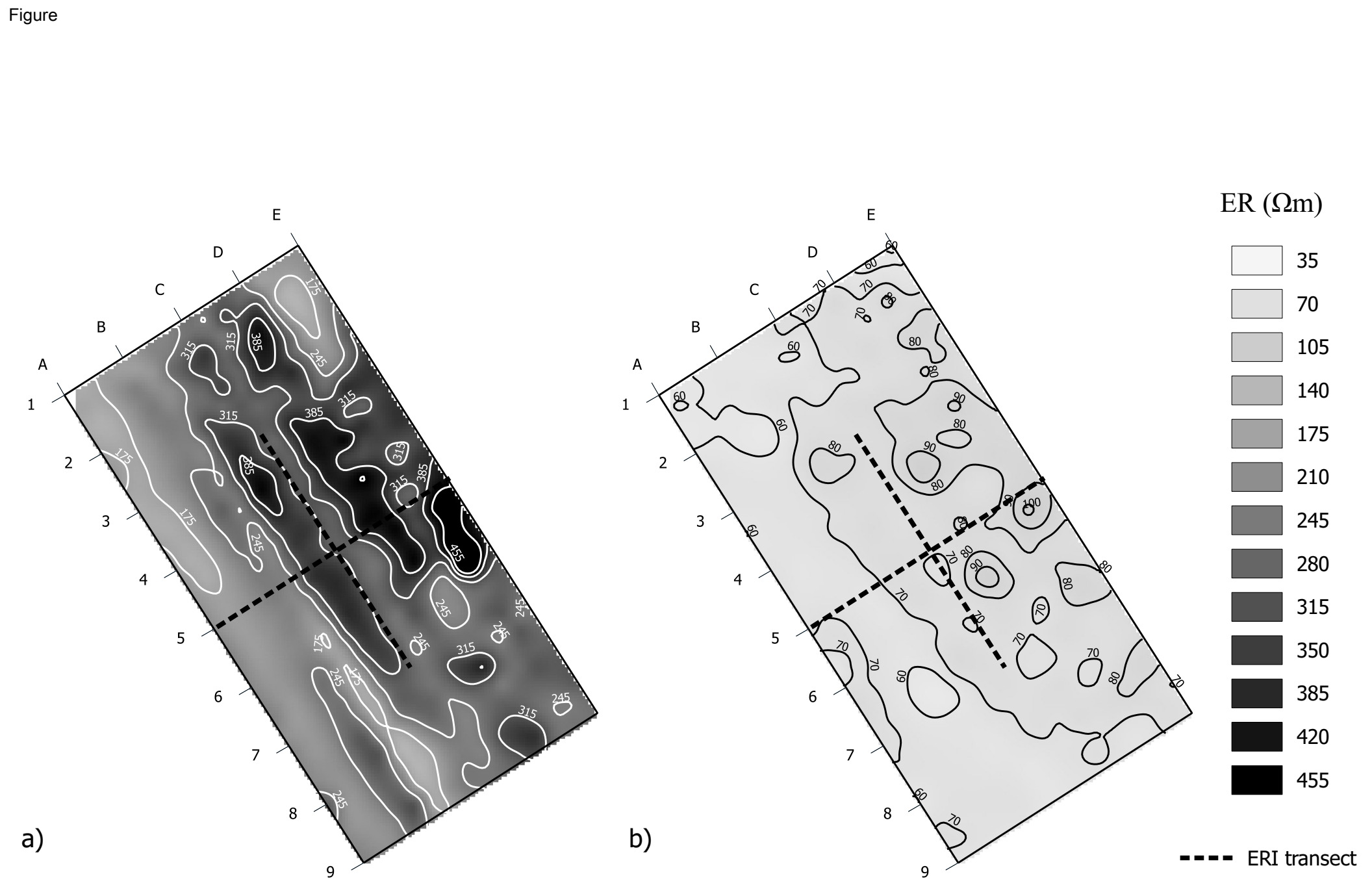
A
B
C
D
E
1
2
3
4
5
6
7
8
9
a)
b)
ER (Ωm)
35
70
105
140
175
210
245
280
315
350
385
420
455
ERI transect

Figure

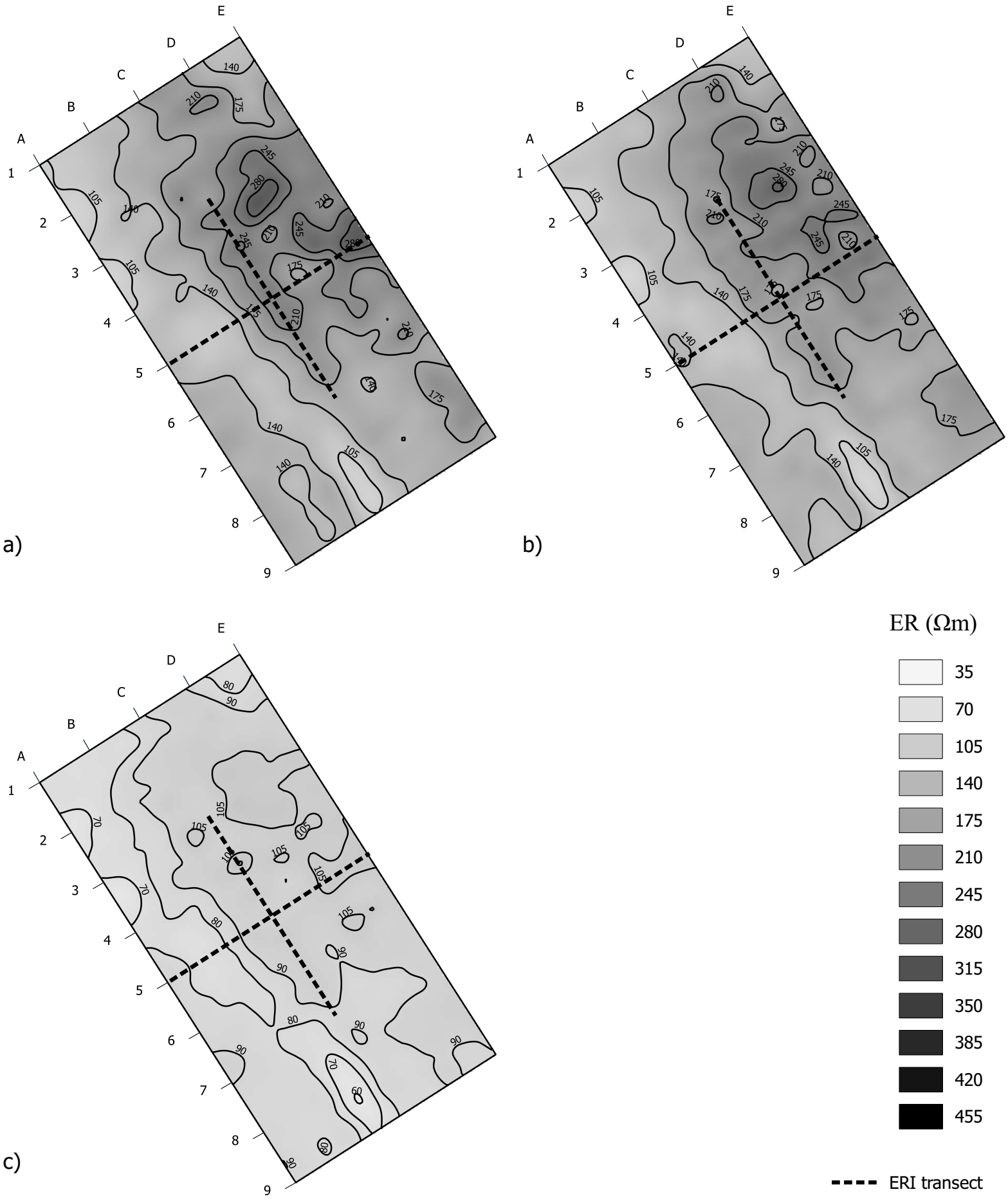
a)
b)
c)
A
B
C
D
E
1
2
3
4
5
6
7
8
9
ER (Ωm)
35
70
105
140
175
210
245
280
315
350
385
420
455
ERI transect

Figure

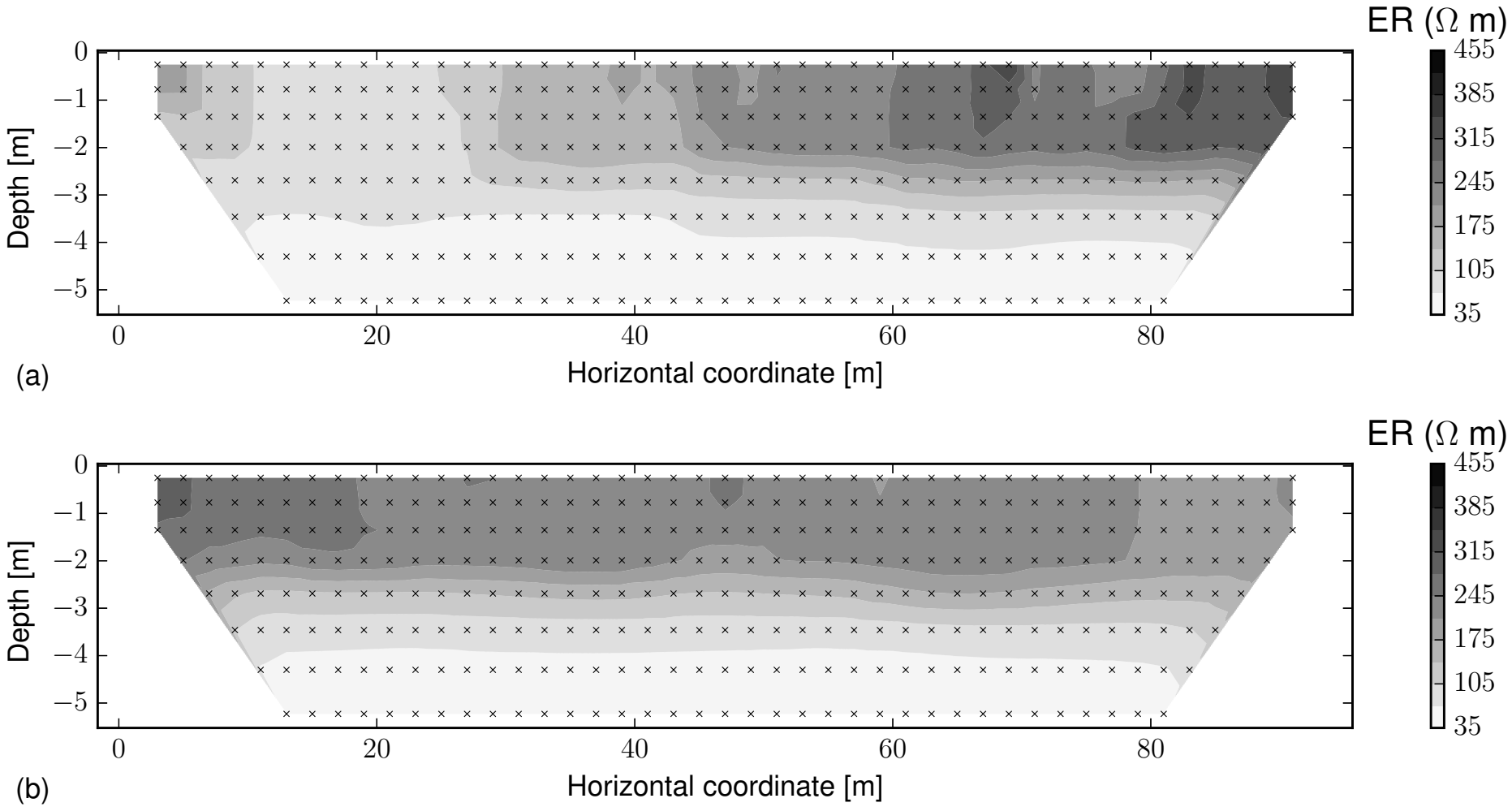
ER (Ω m)
455
385
315
245
175
105
35
Depth [m]
0
−1
−2
−3
−4
−5
0
20
40
60
80
Horizontal coordinate [m]
(a)
ER (Ω m)
455
385
315
245
175
105
35
Depth [m]
0
−1
−2
−3
−4
−5
0
20
40
60
80
Horizontal coordinate [m]
(b)

Figure

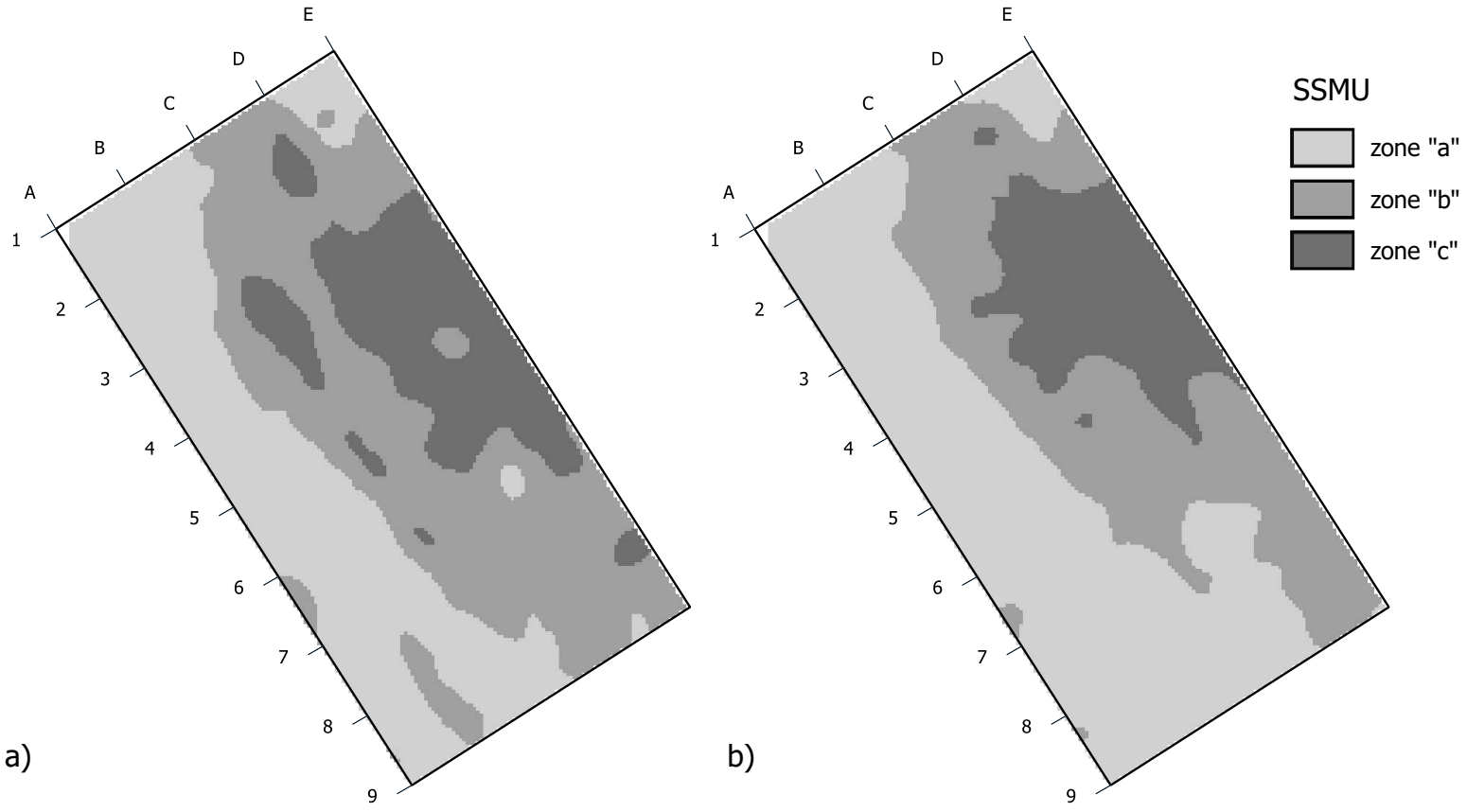
A
B
C
D
E
1
2
3
4
5
6
7
8
9
SSMU
zone "a"
zone "b"
zone "c"

a) b)

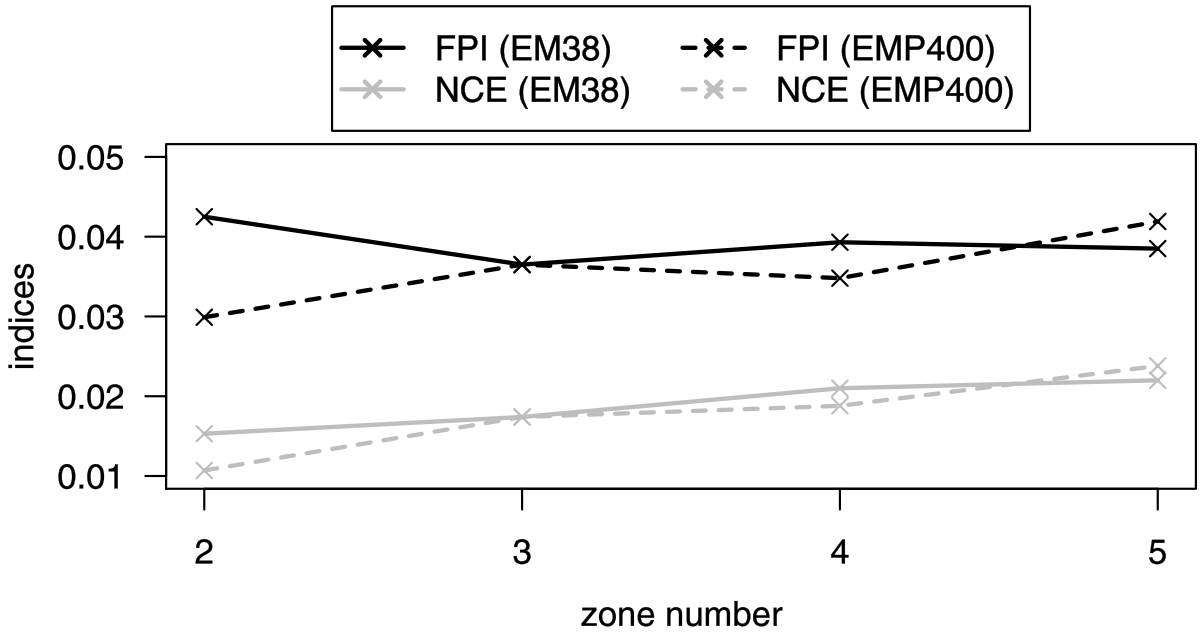
FPI (EM38)
FPI (EMP400)
NCE (EM38)
NCE (EMP400)
indices
0.05
0.04
0.03
0.02
0.01
2
3
4
5
zone number

c)

Figure

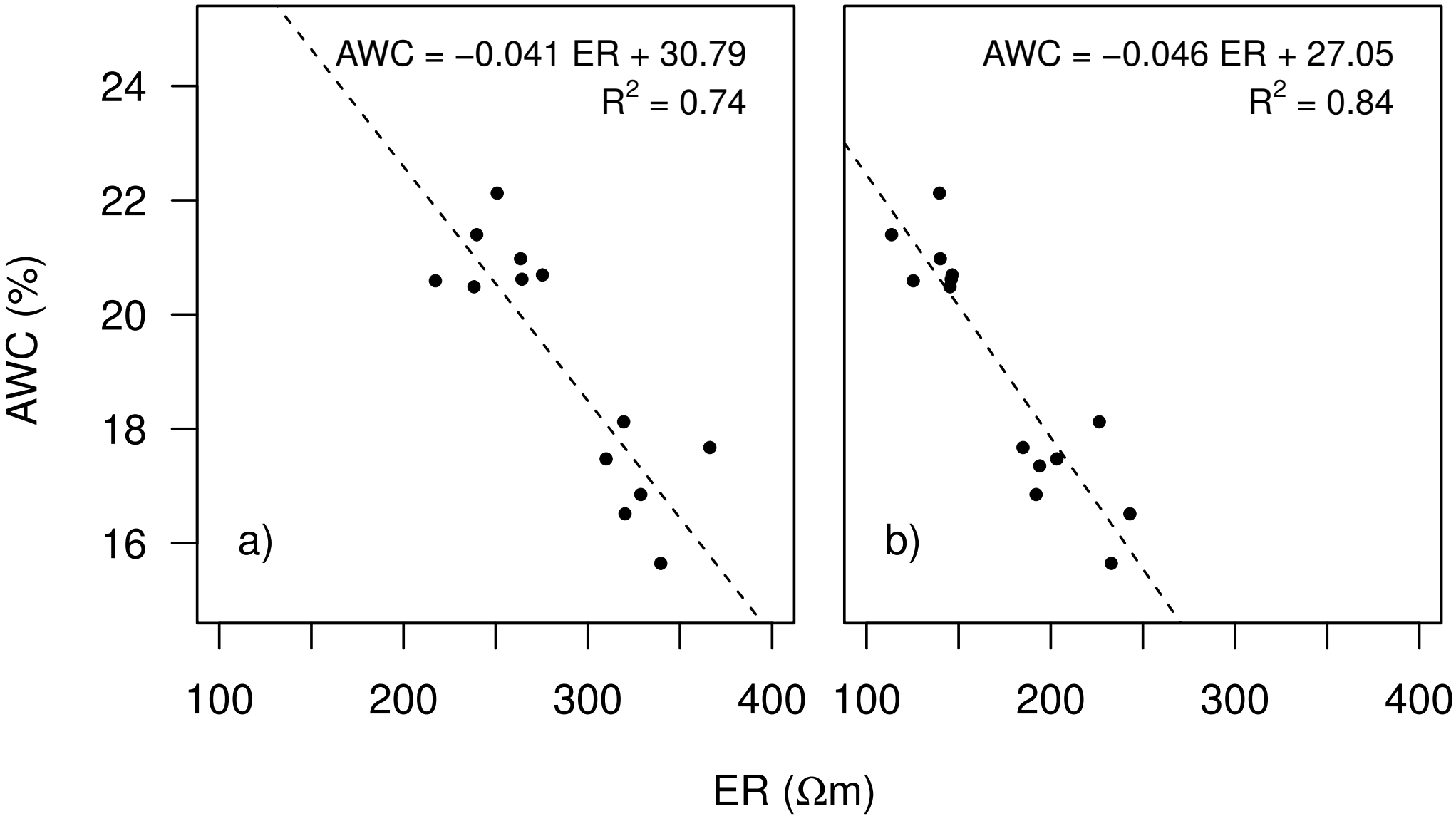
AWC = −0.041 ER + 30.79
R2 = 0.74
AWC = −0.046 ER + 27.05
R2 = 0.84
a)
b)
AWC (%)
ER (Ωm)
16
18
20
22
24
100
200
300
400

Figure

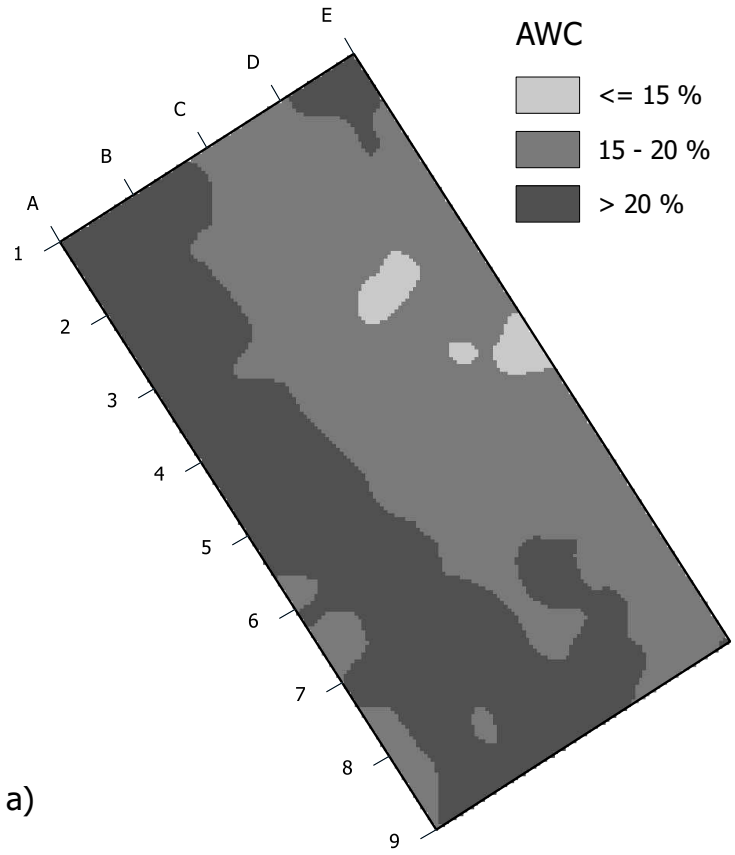
AWC
<= 15 %
15 - 20 %
> 20 %
A
B
C
D
E
1
2
3
4
5
6
7
8
9

a)

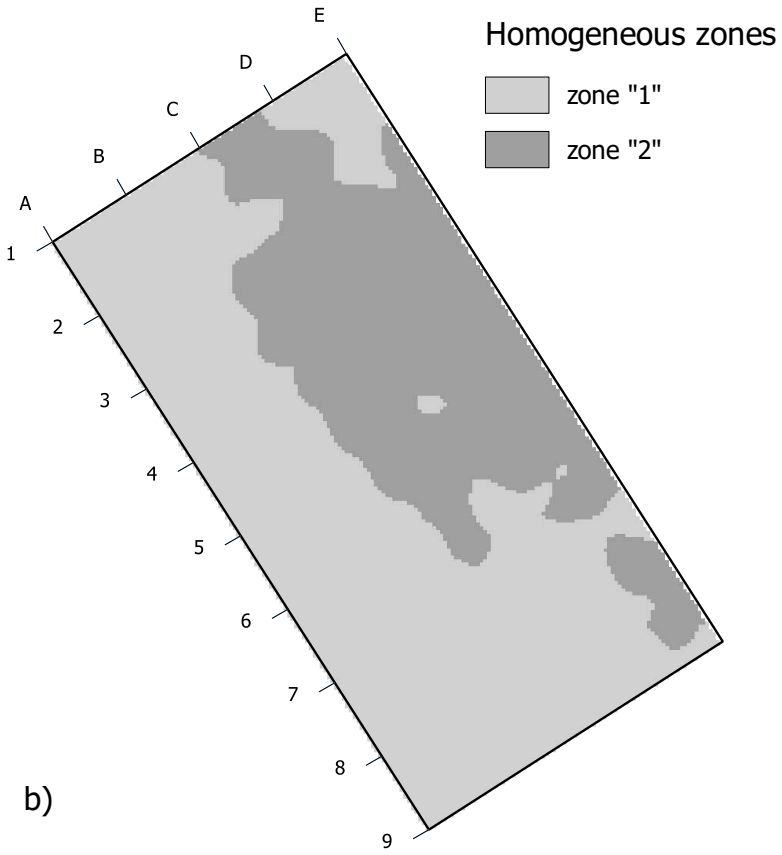
Homogeneous zones
zone "1"
zone "2"
A
B
C
D
E
1
2
3
4
5
6
7
8
9

b)

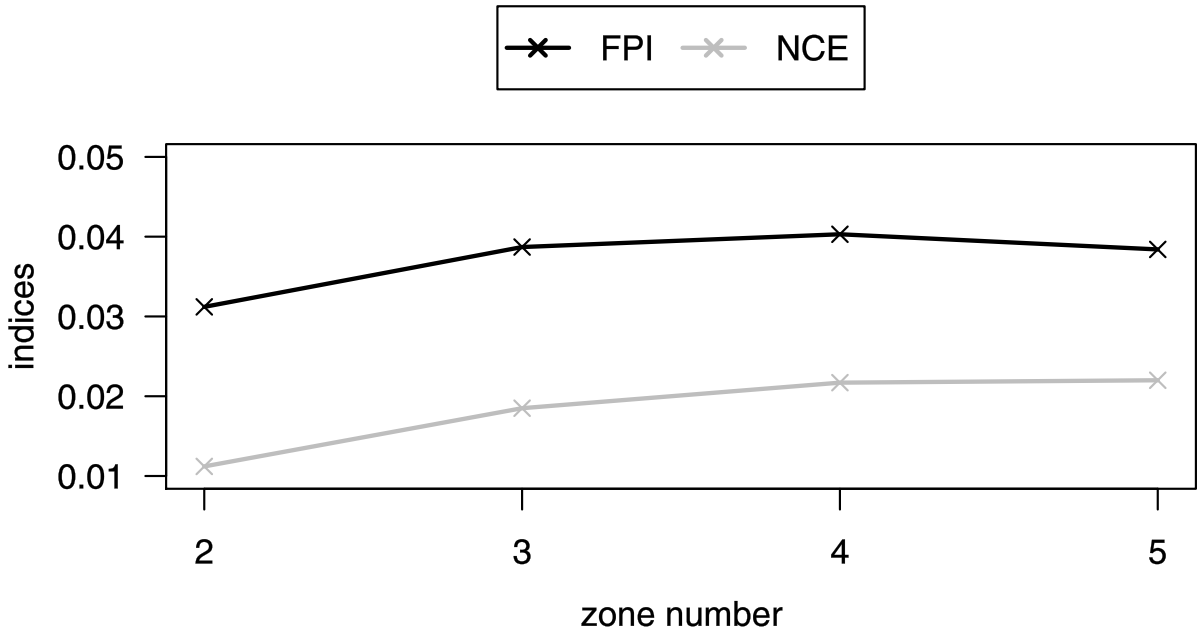
FPI
NCE
indices
0.05
0.04
0.03
0.02
0.01
2
3
4
5
zone number

c)

Figure

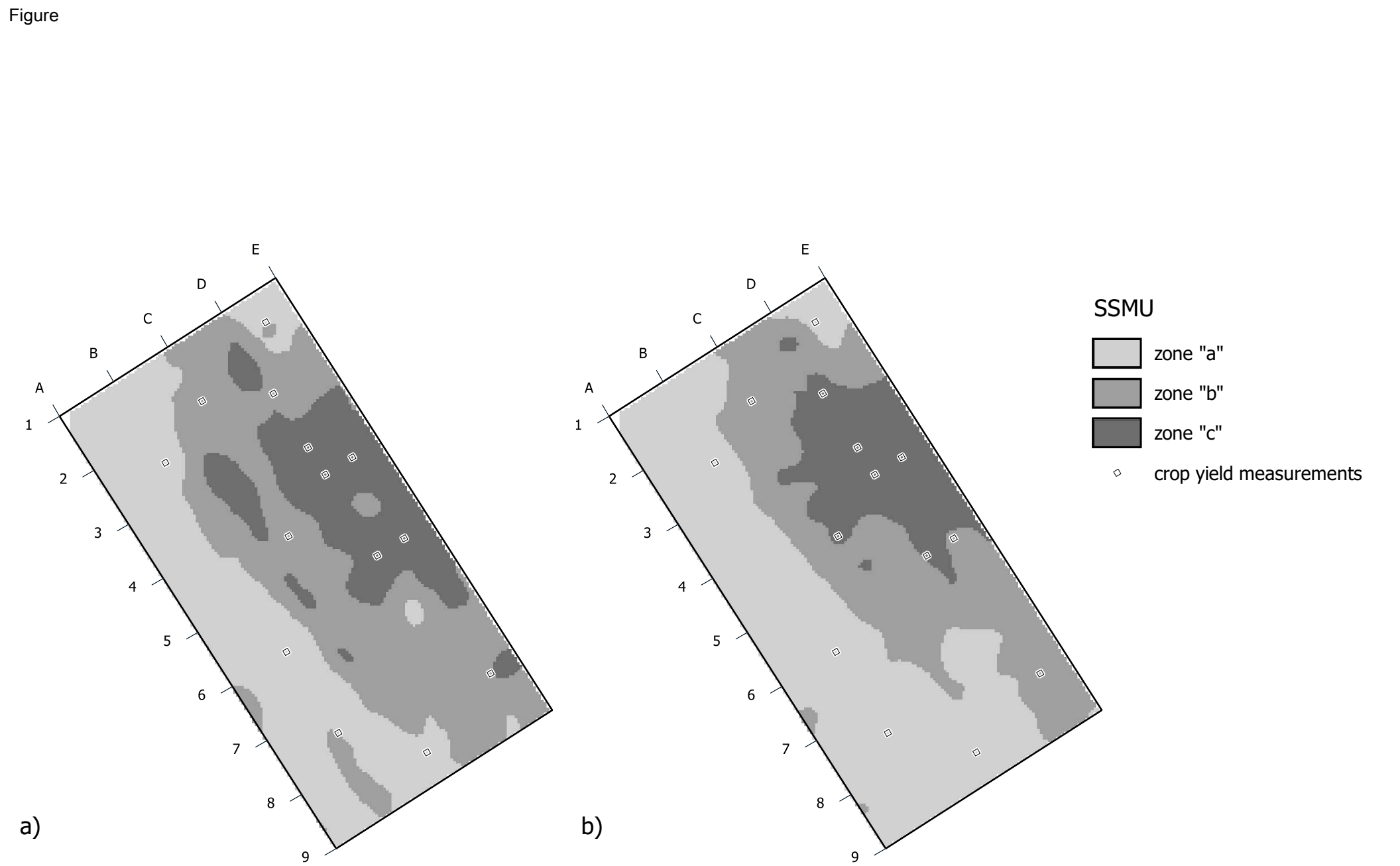
A
B
C
D
E
1
2
3
4
5
6
7
8
9
a)
b)
SSMU
zone "a"
zone "b"
zone "c"
crop yield measurements